Salt-induced fast aggregation of polystyrene latex

M. Carpineti, F. Ferri,* and M. Giglio
Physics Department, University of Milan, via Celoria 16, Milano, Italy

E. Paganini and U. Perini
Centro Informazioni Studi Esperienze Tecnologie Innovative, P.O. Box 12081, Milano, Italy

(Received 27 June 1990)

We study fast, salt-induced aggregation of polystyrene spheres by means of low-angle static light scattering covering two decades of scattered wave vector q. The measurements are taken at a fixed salt concentration, varying the monomer concentration from $c_0=1\times10^9$ to 5×10^{10} cm^{-3}. During each run, the fractal dimension d_f of the clusters and the time evolution of the average radius $\langle R_G\rangle$ and average mass $\langle M\rangle_w$ are determined. At larger concentrations we consistently find $d_f=1.61\pm0.02$, but, as the concentration is decreased, d_f grows to 1.83 ± 0.02. The value of d_f is determined both from the asymptotic behavior of the scattered intensity $I(q)$ and from the relation between the average mass and radius, $I(0)\propto R_G^{d_f}$. Good agreement is found between the two sets of data. The earlier portions of the curves for R_G as a function of time t are compatible with a power-law growth and collapse onto a master curve when the reduced time $T=c_0t$ is used. Noticeable deviations from power-law growth are, however, observed at later times. Finally, we show that for the lowest concentrations the reactions stop when the clusters attain a maximum diameter. We present arguments showing that reaction termination is due to sedimentation, the time required to diffuse across intercluster distance becoming longer than the settling time through the sample due to sedimentation.

I. INTRODUCTION

A substantial amount of work has been produced in the past few years in the area of collodial aggregation, both theoretically and experimentally, especially about the relationship between aggregation dynamic and structure of the aggregates.[1-10] The most widely accepted picture is that there are two limiting behaviors both for the reaction kinetics (and associated evolution of clusters sizes) and for the fractal morphology of the aggregates. The parameter determining which behavior is to be expected is the sticking probability between monomers and between clusters. A sticking probability equal to one leads to the diffusion-limited cluster aggregation (DLCA), while values appreciably smaller than 1 give rise to reaction-limited cluster aggregation (RLCA). These two modes are claimed to be endowed with universality character, and recent papers,[5,10] have shown that quite different types of monomers, metallic colloids, colloidal silica, and polystyrene spheres, do exhibit such universal behavior irrespective of the details of the type of forces responsible for the binding between the monomers.

Accordingly, DLCA clusters have a fractal dimension $d_f\simeq1.8$ and the kinetics is characterized by a power-law growth for the average radius of gyration:

$$R_G\propto t^{1/d_f}\ , \tag{1}$$

while RLCA clusters have a fractal dimension $d_f\simeq2.10$ and the growth is exponential:

$$R_G\propto e^{\alpha t}\ . \tag{2}$$

It should be pointed out that the universal DLCA and RLCA behavior is expected only if well-prescribed and somewhat ideal conditions are met. For example, DLCA is the result of pure diffusion plus a sticking probability equal to 1. Any interaction between parts of clusters in the docking process would make them deviate from purely diffusive motion, thus leading to both reaction kinetics and fractal morphology at variance with the universal scenario. In practice, most aggregating systems are likely to exhibit some degree of cluster interaction, and the predictions of universal DLCA and RLCA have the merit of being the standard against which differences exhibited by more complex systems are gauged.

In fast-aggregation studies d_f is usually determined by static light scattering, since the asymptotic behavior of the scattered intensity $I(q)$ is given by

$$I(q)\propto q^{-d_f}\quad (qR_G\gg1)\ . \tag{3}$$

Conventional static light-scattering systems span roughly one decade in q space, typically between $q=2\times10^4$ and 2×10^5 cm^{-1}.

Aggregation usually takes place so rapidly that only the asymptotic behavior can be ascertained, the $qR_G\simeq1$ region quickly falling outside the observation region. To follow the reaction kinetics, dynamic light scattering is the most commonly used technique. Of course, it would be desirable to obtain information both on d_f and on the kinetics with the same technique and on the same sample.

This possibility is offered by low-angle static light scattering. Since light can be collected even at extremely small angles ($\theta=0.18°$), one can zoom over a substantial q-vector range, typically two decades for the system used in this study to be described in some detail below. We have, therefore, the rather unique opportunity of assessing d_f from Eq. (3), taking advantage of the extended q-vector range and at the same time we can follow the kinetics of aggregation of large clusters.

In this paper we will present results obtained on salt-induced aggregation of polystyrene spheres by means of low-angle static light scattering. The measurements have been taken at a fixed salt concentration and by changing monomer concentration from $c_0=1\times10^9$ to 5×10^{10} particles/cm^3, corresponding to volume fractions $\phi=1.15\times10^{-6}$ and 5.75×10^{-5}, respectively.

The fractal dimension d_f and the time evolution of average cluster radius and mass are determined for each run on still-reacting vessels. For larger values of c_0, d_f is close to 1.61 ± 0.02. As the concentration is decreased, d_f increases, but the data are more erratic. Values up to 1.83 are observed. For the lowest concentrations, the reaction stops once the cluster radius attains a maximum value.

We present arguments showing that termination is due to the fact that the time to diffuse across intercluster distances becomes larger than the settling time through the sample due to sedimentation.

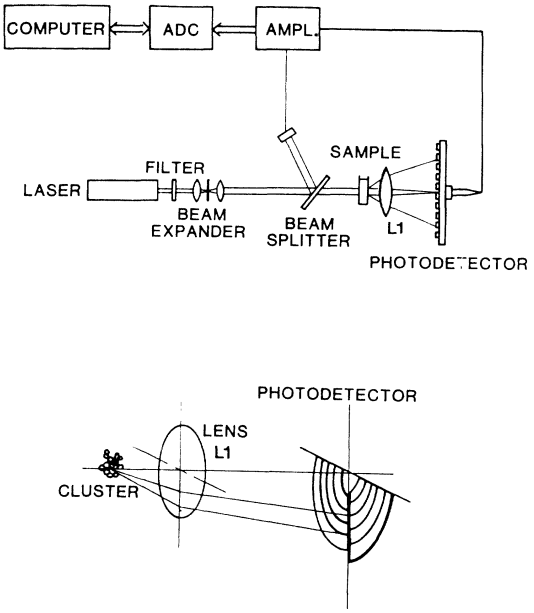

FIG. 1. The experimental setup. The geometry of the sensor elements is only qualitatively depicted here. The average radii of the 31 elements scale according to a geometric law.

II. EXPERIMENTAL METHODS

The setup is shown in Fig. 1. A collimated, vertically polarized He-Ne laser beam falls onto a cuvette and the transmitted beam, together with the scattered light, is collected by the lens L1. A 31-element solid-state sensor is placed in the focal plane of L1. Each element is shaped as one quarter of an annulus. The average radii of the elements are scaled according to a geometric law, so that the corresponding scattering wave vectors are equispaced on a log plot. The ranges of scattering angles θ and wave vectors q are $0.18°\le\theta\le12.1°$ and 4×10^2 cm$^{-1}\le q\le3\times10^4$ cm^{-1}, respectively.

On center a tiny hole allows the transmitted beam to pass clear of the sensing elements. A separate detector measures the transmitted beam power behind the multielement sensor. Also, an additional sensor is placed so as to monitor the power of the main beam via a beam splitter before the scattering cell. In this way the turbidity of the sample can be determined, and incoming beam fluctuations are monitored. The multielement sensor annuli are shaped so to occupy only a half plane on the sensor surface (see Fig. 1). The scattering cuvette is slightly canted so that the image of the back reflection of the focused beam spot is diverted to the blind area of the sensor plane. The lens L1 is coated with high-quality antireflection coatings, the residual single surface reflection being less that 3% for all the scattering angles.

All the scattered light sensors and the two beam monitors are read in sequence with an interface with a personal computer. The time required to obtain a set of data for 31 angles is less than 100 msec, a time shorter than any characteristic time constant of the aggregation process. The analog-to-digital card has a software controlled gain setting in order to cope with the great dynamic range of the signals.

It is important to point out that, with the optical layout in Fig. 1, any light, including stray light from the cuvette spots, is brought to the sensor. We therefore take blank measurements with the cell filled with filtered deionized water prior to any run. In order to properly subtract the stray-light contributions, the blank measurements are adjusted taking into account both the incoming beam power and the sample turbidity. To reduce the effects of the stray light, we select cuvettes with an optical path that guarantees that the overall extinction due to sample scattering amounts to a few percent. $I(q)$ is normalized to the transmitted intensity, so as to account for the sample turbidity. Sample turbidity corrections, however, are almost irrelevant, since turbidity is small anyway and changes very little once the cluster radii fall in the measuring range of the apparatus.

We should point out that with the setup shown in Fig. 1, the annular detectors collect light out of the scattering plane, and in principle one should worry about dipole corrections. However, since the largest average scattering angle θ is roughly 12°, the dipole $\sin^2(\phi)$ dependence can be ignored. In fact, taking into account the shape of the sensors, the ϕ angle for the outermost element varies from 78° to 90°. When the $\sin^2(\phi)$ dependence is averaged over the outermost element, the required correction would be of the order of 2%. Of course, smaller corrections are necessary for the inner elements. We therefore conclude that the out-of-plane dipole corrections are

comparable to or smaller than the typical experimental uncertainty in the readings of the scattered intensity. Furthermore, such small corrections would lead to unappreciable changes in the estimate of the fractal dimension via Eq. (3).

III. SAMPLE

Polystyrene spheres were chosen to fully exploit the potentialities of the low-angle static light-scattering technique. Indeed the price to pay for working at extremely small angles is that it is virtually impossible to avoid spurious contributions due to stray light coming from the spots at the entrance and exit windows of the scattering cell. Though blank measurements and incoming beam monitoring are used to compensate for these effects, it is necessary that the total amount of light scattered by the sample is at least a few percent of the incoming beam. When using small-diameter monomers, as we did in a previous study on Ludox,[11] the minimum number concentration we could utilize was already pretty large. Since the time constant which controls the pace at which the reaction proceeds is given by[12]

$$\tau_0=\frac{3\eta}{4k_bT}\frac{1}{c_0}\ , \tag{4}$$

the concentration range over which one can work is rather limited because as the concentration is increased, the reaction becomes so fast that one has difficulties in following the kinetics.[11] A scant factor of 5 in concentration could be explored in the Ludox study.

Larger spheres allow more flexibility, and one can work in the DLCA mode keeping τ_0 conveniently long, since even for rather low values of c_0 the scattered signals are large enough to be analyzed with our instrument. In this study we have used polystyrene spheres of radius $R_0=0.065\ \mu$m.

Taking into account that their index of refraction is $n_{\text{spheres}}=1.58$ and that they are suspended in water ($n_{\text{water}}=1.33$), the Rayleigh-Gans conditions

$$|m-1|\ll 1\ , \tag{5a}$$

$$\frac{2\pi}{\lambda}a|m-1|\ll 1 \tag{5b}$$

are fairly well satisfied ($m=n_{\text{spheres}}/n_{\text{water}}$).

The scattered intensity by monomers is given by[13]

$$I_{\text{monomers}}(q)\sim|m-1|^2\frac{9\pi}{3(qR_0)^3}J^2_{3/2}(qR_0)\ . \tag{6}$$

Equation (6) gives a fractional variation of the scattered intensity between the smallest and the largest q value spanned by the instrument of less than 2%. We can therefore ignore any effect due to the form factor when analyzing the scattered intensity distribution from the clusters. To check experimentally the validity of this assumption, we have taken measurements on a nonaggregating sample. Due to the small diameter of the monomers, the signals out of the innermost sensors were rather weak. The 10–15 outermost sensors, however, gave signals strong enough to clearly indicate that the intensity distribution was flat over that region. As an additional test, the same sample was also studied by dynamic light scattering at 90° using a Brookhaven 2030AT. The analysis of the data with non-negatively constrained least-squares fit gave an average sphere diameter of $0.139\pm0.022\ \mu$m, in very good agreement with the manufacturer specification ($0.130\pm0.031\ \mu$m). This confirms that the size of the spheres was indeed small and no appreciable aggregation was present. All these results further justify that the form factor can be taken as constant and therefore $S(q)$ is proportional to $I(q)$.

The monomers have corboxyl groups on the surface. They are carefully treated to make them surfactant free via cleaning with exchange resins,[14] since it has been pointed out that the presence of surfactant may change the nature of the two-particle potential.[15]

The samples are made by preparing two beakers containing outgassed filtered water. In the first beaker we introduce the monomers and in the second we add the salt. The contents of the beakers are then mixed together. By so doing we try to avoid either salt or monomer concentration shocks during the preparation. Of course, salt and monomer concentration in the original beakers were chosen so that the final composition after mixing was the desired one. Monomer concentration was varied between $c_0=1\times10^9$ monomers/cm^3 and $c_0=5\times10^{10}$ monomers/cm^3. The salt used was $MgCl_2$. All the runs have been made to a fixed salt concentration, namely 30 mM. The salt concentration was chosen to be large enough to assure fast aggregation, as confirmed by visual inspection of a series of reacting vessels prepared at various salt concentrations. Incidentally, the critical concentration estimated on the basis of the Derjaguin, Landau, Verwey, and Overbeek theory[12,15] and the known characteristics of the spheres are in fair agreement with the value determined empirically.

IV. EXPERIMENTAL RESULTS

Figure 2 shows a few intensity distributions $I(q)$ taken during a run at monomer concentration $c_0=1.5\times10^{10}$. At the earlier stages one can notice the typical behavior with the rolloff corner at $q=1/R_G$ and the asymptotic power-law decay q^{-d_f} at larger q. One can also notice at later times that the asymptotic behavior is displayed over the entire q range accessible to the instrument. This allows a rather accurate estimate of the fractal dimension. Furthermore, all the curves fall at large q onto the same asymptotic line. It can be easily shown that this is a consequence of the conservation of mass within the scattering volume, and that implies that no loss due to sedimentation had actually occurred.

In fact, if we take for $S(q)$ the usual Fisher-Burford expression[16]

$$S(q)=\frac{S(0)}{[1+(qR_G)^2/\frac{3}{2}d_f]^{d_f/2}}\ , \tag{7}$$

taking the limit for $qR_G\gg1$ and taking into account that

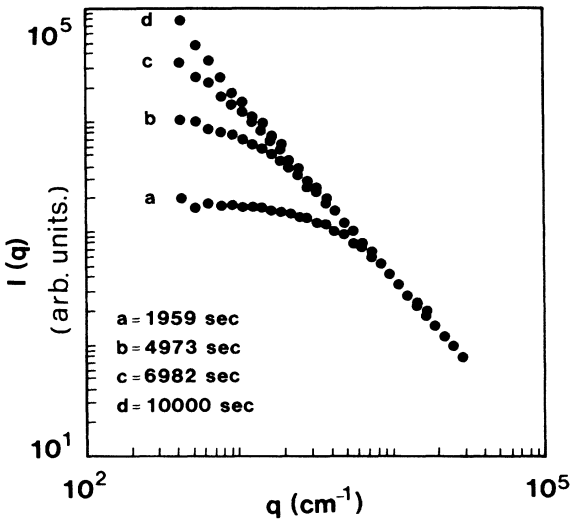

FIG. 2. Typical log-log plot of $I(q)$ collected at various times during the run at $c_0 = 1.5 \times 10^{10}$ cm^{-3}.

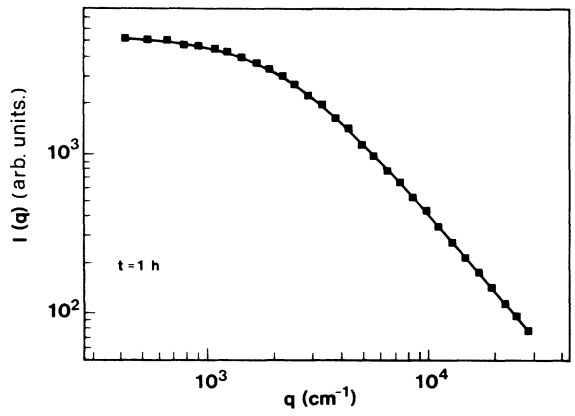

FIG. 3. Typical result of a nonlinear least-squares fit of experimental data with a Fisher-Burford function.

a fractal aggregate of radius R_G has a mass M,

$$M(R_G) = m_0 \left[\frac{R_G}{R_0} \right]^{d_f} , \tag{8}$$

where R_0 and m_0 are the monomer radius and mass, respectively, we have

$$I(q) \propto q^{-d_f} \int N(R_G) M^2(R_G) R_G^{-d_f} dR_G . \tag{9}$$

We then find

$$I(q) \propto M_{\mathrm{TOT}} \frac{m_0}{(qR_0)^{d_f}} \quad (qR_G \gg 1) . \tag{10}$$

All the distributions $I(q)$ collected during the various runs have been fitted via a nonlinear least-squares fit[17] using the Fisher-Burford expression. A typical result of the fitting procedure is shown in Fig. 3. The solid line is the fit obtained by floating the extrapolated $I(q=0)$ value, the average radius of gyration, and the fractal dimension d_f.

It is to be pointed out that out of many hundreds of curves examined, none seemed to show significant deviation from the form given by Eq. (7), provided that the sample is left reacting in the cuvette. We also found that even delicate manipulations of the sample lead to deviations from fractal morphology or to an apparent growth of the fractal dimension. We tried to transfer the samples from the beaker, where they were reacting, to the cuvette and we found different values for the fractal dimension. All these values were greater than that of the sample grown in a stationary mode in the cuvette (see Fig. 4). The effect becomes even more pronounced if the transfer is done via a syringe with a needle. Stronger shears seem to give more pronounced effects. We have found that also dilution, although commonly used, can damage the aggregates forcing the fractal dimension to grow (see Fig. 5). We have therefore decided to perform runs only on still reacting cuvettes.

Except for the very lowest concentrations used, the duration of each run is determined by the time required to observe straight lines in the log plot of $I(q)$. It varies from a few hours to a few days.

For each run we can extract the value of the fractal dimension from the terminal curves like curve d in Fig. 2. Also, with the nonlinear least-squares fit, we determine the time evolution of the average cluster radius and of the intercept at $q=0$ which is proportional to the weight average molecular weight. Furthermore, since the fractal dimension is kept floating in the fit, we also have estimates of d_f as the reaction proceeds.

In Fig. 6 we show the value of the fractal dimension as a function of monomer concentration. For the larger values of the concentration d_f is very stable and close to

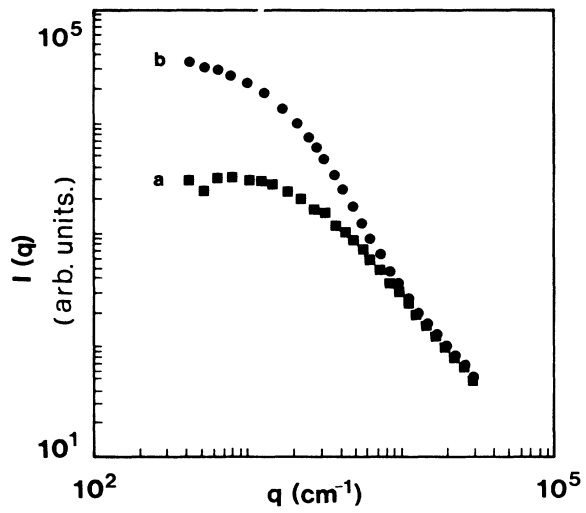

FIG. 4. Example of shear-induced distortions caused by the transfer of a sample from a reacting vessel to the scattering cuvette (curve b). Curve a is the $I(q)$ for the same sample grown undisturbed in the scattering cuvette.

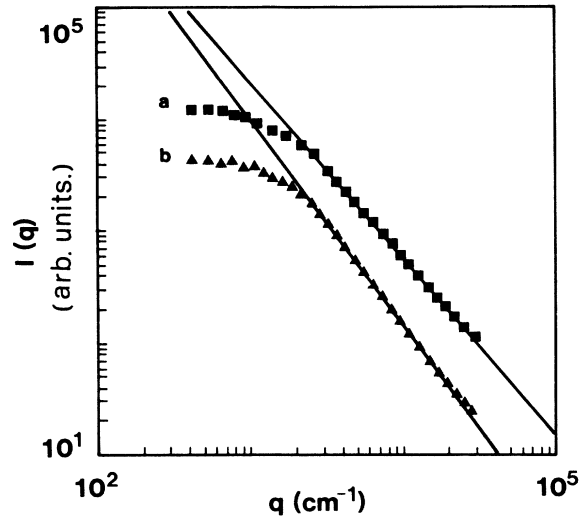

FIG. 5. Distortions caused by diluting a sample growing in the scattering cuvette. The sample was diluted by a factor of 4 by adding pure water. Curve *a* is the undiluted sample, curve *b* is after dilution.

1.60. The results are quite reproducible from run to run.

At smaller values of the concentration, the fractal dimension starts to increase as c_0 is reduced, and the results become more erratic. Values as high as 1.83 are observed.

Let us first discuss the $d_f = 1.6$ result. It is a low value when compared with the DLCA value $d_f \simeq 1.8$. Multiple scattering is the most obvious source of trouble one could think of to explain the difference, and therefore this matter has to be treated carefully. Indeed, multiple scattering in metallic colloids was claimed[4] to be responsible for spurious reduction of fractal dimension as extracted from asymptotic $I(q)$ curves.

Due to the peculiar optical arrangement for our low-angle static light-scattering technique, the amount of multiple scattering can be varied by changing the thickness of the sample. We have therefore performed runs at the same concentration $c_0 = 2\times10^{10}$ cm^{-3}, but using cells of 2-, 5-, and 10-mm optical paths. The beam extinction close to the end of each run changed accordingly from 6% to 30%. It should be stressed that in analogy with scattering from critical systems, the turbidity tends to saturate when $q_{\text{backscattering}} R_G \gg 1$, so we do not have to worry about the exact value of the elapsed time at which the measurements were taken. The fractal dimension we determined was $d_f = 1.59$, 1.60, and 1.60, respectively, for the three cells, thus providing a strong indication that multiple scattering is not effective in our measurements.

A further element to be considered is that the same set-up used for this study gave values for d_f quite consistent with the universal values in the previous Ludox study.[11] Incidentally, the beam attenuation values in the runs with colloidal silica fell pretty much in the range of the test described above.

Finally, we want to remark that some older measurements[18] on polystyrene spheres 0.085 μm in diameter gave a value $d_f = 1.61$, in agreement with our results.

To further corroborate the estimates of d_f obtained from terminal curves of $I(q)$, we have also plotted on a log-log plot the behavior of $I(0)$ versus average radius, since $\langle M \rangle_w$ is proportional to $R_G^{d_f}$. Data are shown in Fig. 7 for $c_0 = 2\times10^{10}$ and 1×10^9 cm^{-3}. One can notice that the power-law behavior is remarkably good. We report in Table I the comparison between the estimates of d_f from the asymptotic behavior of $I(q)$ and from the slope of the curve of $\langle M \rangle_w$ versus R_G.

The agreement between the two sets of data is fairly

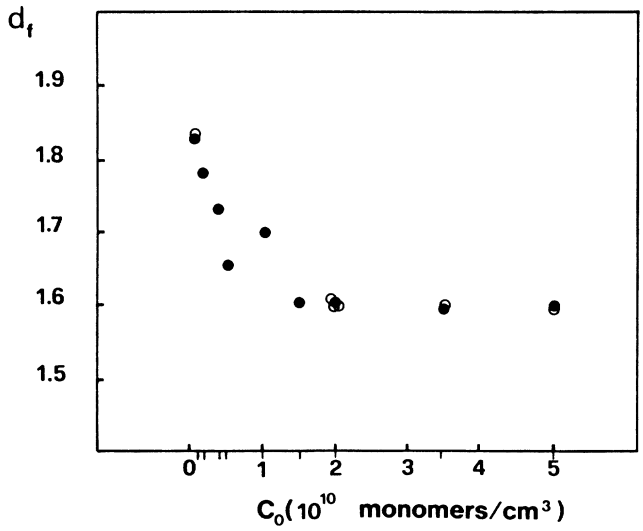

FIG. 6. Behavior of the fractal dimension [as obtained from the asymptotic $I(q)$ behavior] as a function of monomer concentration.

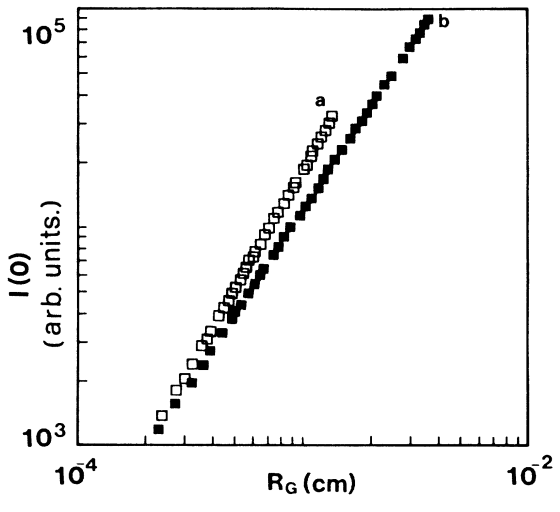

FIG. 7. Log-log plot of $\langle M \rangle_w$ [$I(0) \propto \langle M \rangle_w$] vs R_G for two values of the concentration: $c_0(a) = 1\times10^9$ cm^{-3}, $c_0(b) = 2\times10^{10}$ cm^{-3}. The slope gives an independent estimate of d_f.

TABLE I. Comparison between the d_f values extracted from asymptotic behavior of $I(q)$ as in Fig. 2 (column a) and those extracted from $\langle M \rangle_w$ vs R_g (column b).

C_0	d_f (a)	d_f (b)
1×10^9	1.83	1.85
2×10^9	1.78	1.78
4×10^9	1.73	1.72
5×10^9	1.65	1.55
1×10^{10}	1.70	1.69
1.5×10^{10}	1.60	1.60
2×10^{10}	1.61	1.58
3.5×10^{10}	1.59	1.58
5×10^{10}	1.60	1.57

good, thus further supporting the evidence that indeed the fractal dimension changes as the concentration is varied.

We now discuss the growth of the average radius as a function of time. In Fig. 8 we show a few time evolutions plotted against $T=c_0t$, where c_0 is the number concentration and t the time in sec. Indeed, according to the elementary diffusion-controlled aggregation theory,[12] a change in the monomer concentration changes the characteristic time scale for the kinetics [see Eq. (4)], and all the curves should superimpose once one uses the reduced time scale. As one can notice, this is pretty much the case for the curves shown in Fig. 8. As a general feature, one can notice that in the initial portion, the curves are indeed fairly well superimposed and compatible with a power-law growth. The quality of the data unfortunately allow us to extract only a crude estimate of the exponent characterizing this initial portion of the curves. Loosely speaking, taking into account the large error in this estimate, the value of d_f obtained from Eq. (1) is compatible with the range of values listed in Table I. We are not in the position of making any stronger statement also because, at later times, the curves tend to roll upwards and the transition point is ill defined, shifting to smaller values of c_0t as the monomer concentration is reduced.

Finally, we want to discuss an anomalous behavior observed in the kinetics for the lowest concentrations $c_0=1\times10^9$ and 2×10^9 cm^{-3}. In both cases the average cluster radius stops growing after attaining a maximum diameter of 15–20 μm. We show in Fig. 9 the final portion of the evolution at $c_0=1\times10^9$ cm^{-3}. As one can notice, after the attainment of the maximum diameter, sedimentation sets in and material is lost from the scattering volume at later times. We point out that, to our knowledge, premature termination of fast aggregation has never been observed before. The fact that it is observed in this experiment is associated with the exceptionally large clusters that can be studied with our instrument.

According to the scheme described below, similar effects should be observable even at higher concentrations, provided one could explore even smaller regions in q-vector space. The explanation that we present below is based on comparison between typical aggregation time constants of large clusters and the time required to sediment over the height of the sample. A cluster of radius R_G and of fractal dimension d_f is made up by n monomers according to the following relation

$$n=(R_G/R_0)^{d_f} , \tag{11}$$

where R_0 is the monomer radius.

Since in fast aggregation, narrow-band distributions are expected, we can calculate the time constant for cluster aggregation using the expression for diffusion aggre-

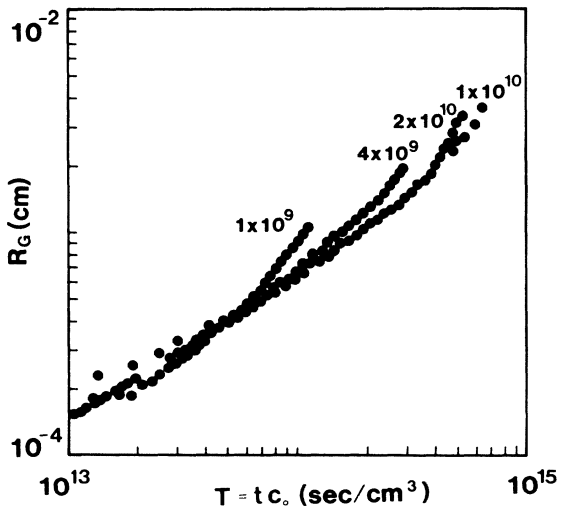

FIG. 8. Evolutions of R_G as a function of $T=tc_0$ for different values of c_0.

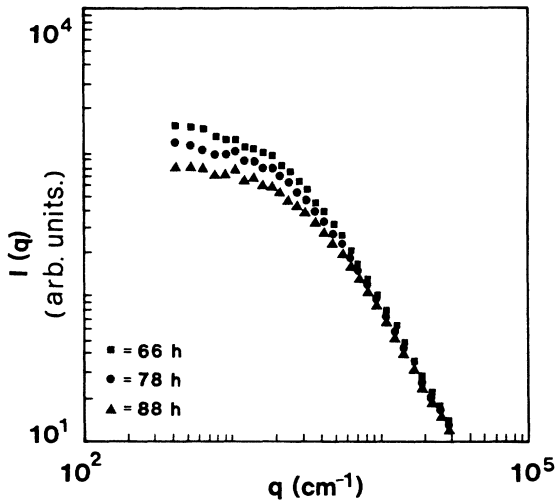

FIG. 9. Evidence of premature termination of the aggregation process for $c_0=1\times10^9$ cm^{-3}. Notice sedimentation effects evidenced by the fact that curves tend to shift downwards as time proceeds.

gation between spheres:[12]

$$\tau_{\rm agg}=\frac{3\eta}{k_bT}\frac{1}{c_{\rm cluster}}=\frac{3\eta}{k_bT}\frac{1}{c_0}\left[\frac{R_G}{R_0}\right]^{d_f}, \tag{12}$$

where $c_{\rm cluster}$ is the number concentration of the clusters of radius R_G.

We can then ask how long it would take for such a cluster to sediment across the height of the cuvette (or beaker). We will assume that the clusters are not free draining, and therefore the sedimentation velocity is given by

$$v_1=\frac{2R_0^2 g(\rho_2-\rho_1)}{9\eta}\left[\frac{R_G}{R_0}\right]^{d_f-1} \tag{13}$$

with ρ_1 and ρ_2 being respectively, the water and the polystyrene density. Accordingly, the time to sediment over a height h is

$$\tau_{\rm sed}({\rm sec})=\frac{9h\eta}{2R_0^2 g(\rho_2-\rho_1)(R_G/R_0)^{d_f-1}}\ . \tag{14}$$

Notice that as R_G grows, $\tau_{\rm agg}$ increases, while $\tau_{\rm sed}$ gets smaller. So, for a given choice of R_G and h there will be a concentration c_0 that will satisfy the relation

$$\frac{\tau_{\rm agg}}{\tau_{\rm sed}}=\left[\frac{R_G}{R_0}\right]^{2d_f-1}\frac{R_0^2 g(\rho_1-\rho_2)}{6k_BTh}\frac{1}{c_0}\simeq 1\ . \tag{15}$$

Under such circumstances, the clusters have grown so large that they are so sluggish in their diffusive motion as to have little chance to come in contact before they actually fall to the bottom of the container. One expects severe deviations from the theoretical expectations based on diffusive motion.

For our experimental condition, taking $d_f=1.65$ and $c_0=1\times10^9$ monomers/cm^3 we find that Eq. (8) is satisfied if $15<R_G<20\ \mu$m. In order to test the validity of the explanation given above, we have performed two runs using an isopicnic solution obtained by mixing water and heavy water so as to match the monomers density.

A first run was made at $c_0=2.5\times10^{10}$ cm^{-3}, so as to perform a control measurement in a region where sedimentation effects should be of no relevance. A straight line for $I(q)$ in the log-log plot was observed, the fractal dimension being $d_f=1.61$, in good agreement with the previous results.

The second run was at $c_0=2\times10^9$ cm^{-3}. Data were collected over 4 d. No sign of sedimentation was evident and fractal dimension $d_f=1.86$ was observed.

We conclude that, indeed, the premature termination of the kinetics is a consequence of sedimentation effects. Also, the growth of d_f at small values of c_0 does not appear to be connected with sedimentation.

V. CONCLUSIONS

The use of our low-angle static light scattering, covering a range of scattered wave vectors almost ten times larger than that accessible with conventional systems, has allowed us to perform an accurate analysis of the fractal dimension of clusters of polystyrene spheres grown under salt-induced aggregation. The data show unambigously that the clusters are remarkably good fractals, and their dimension d_f changes from $d_f=1.60\pm0.02$ to 1.83 ± 0.02 as the concentration of monomers is reduced.

Almost the entire range of d_f observed falls below the universal DLCA value $d_f\simeq1.8$. It should be stressed that the DLCA value was indeed observed[5] for polystyrene spheres, but the aggregation was then induced by neutralizing surface charges on the monomers by addition of HCl, rather than screening the charges via counterions as we did in this work.

Apparently charge neutralization makes the aggregation much closer to the idealized DLCA conditions. Indeed, preliminary measurements, on salt-induced aggregation have shown deviations from DLCA.[19]

Counter ion screening probably makes the clusters polarizable due to electrostatic force, and simulations by Jullien[20,21] have shown that this leads to a reduction of d_f, since sticking on tips is emphasized. A reduction of d_f from the theoretical DLCA value was indeed reported[22] for two two-dimensional aggregations of silica microspheres.

The pronounced vulnerability of our clusters to shear disturbances is also to be tentatively ascribed to the residual electrostatic cluster interaction, while the polystyrene clusters grown with HCl seem to be more rigid than those studied in this work.[19]

As to the reaction kinetics we again report deviation from DLCA behavior, though we find quite reassuring the observation that the data for R_G versus reduced-time c_0t group together fairly well onto a master curve, in spite of the fact that c_0 is varied by a factor of 50. Further comments on the kinetics could only be made in the light of future and highly needed simulation work, which would explicitly take into account deviations from the pure DLCA mode.

While DLCA will remain the only and safe main reference frame against which to compare the zoology of results obtained with more complex systems, we feel that the area of colloidal aggregation is still a quite lively and open field of investigation. Indeed, this work shows that it does not take too much to slip away from the pure DLCA scenario.

ACKNOWLEDGMENTS

We are greatly indebted to D. A. Weitz and R. Klein for illuminating conversations and encouragement. D. A. Weitz is also thanked for bringing to our attention the works by R. Jullien. We also acknowledge with thanks constructive and clarifying discussions and correspondence with D. S. Cannell and D. Schaefer. We wish to express our gratitude to J. Serra of Biokit, Barcelona, for his continuous supply of surfactant free polystyrene latex and z-sizer measurements. Thanks are also due to O. Cremonesi for help with the CERN MINUIT nonlinear least-squares fitting program, to L. D'Arcio and D. Asnaghi for technical problems and isopicnic measurements, and to L. Cantù for dynamic light-scattering measurements. This work has been supported by Centro Nazionalo Ricerche, Gruppo Nazionale di Elettronica Quantistica e Plasmi, and Ministero Università Ricerca Scientifica e Technologica grants.

*Present address: Department of Physics, University of California, Santa Barbara, CA 93106.

[1]D. W. Schaefer, J. E. Martin, P. Wiltzius, and D. S. Cannell, Phys. Rev. Lett. **53**, 2371 (1984).

[2]D. A. Weitz, J. S. Huang, M. Y. Lin, and J. Sung, Phys. Rev. Lett. **53**, 1657 (1984).

[3]M. Y. Lin, H. M. Lindsay, D. A. Weitz, R. C. Ball, R. Klein, and P. Meakin, Phys. Rev. Lett. **54**, 1416 (1985).

[4]J. P. Wilcoxon, J. E. Martin, and D. W. Schaefer, Phys. Rev. Lett. **58**, 1051 (1987).

[5]M. Y. Lin, H. M. Lindsay, D. A. Weitz, R. C. Ball, R. Klein, and P. Meakin, Proc. R. Soc. London Ser. A **423**, 71 (1989).

[6]J. P. Wilcoxon, J. E. Martin, and D. W. Schaefer, Phys. Rev. A **39**, 2675 (1989).

[7]P. Meakin, in *The Fractal Approach to Heterogeneous Chemistry,* edited by D. Avnir (Wiley, New York, 1989), Chap. 3, pp. 140–144.

[8]B. J. Olivier and C. M. Sorensen, Phys. Rev. A **41**, 2093 (1990).

[9]J. E. Martin, J. P. Wilcoxon, D. W. Schaefer, and J. Odinek, Phys. Rev. A **41**, 4379 (1990).

[10]M. Y. Lin, H. M. Lindsay, D. A. Weitz, R. C. Ball, R. Klein, and P. Meakin, Phys. Rev. A **41**, 2005 (1990).

[11]F. Ferri, M. Giglio, E. Paganini, and U. Perini, Europhys. Lett. **7**, 599 (1988).

[12]P. C. Hiemenz, in *Principles of Colloid and Surface Chemistry,* edited by J. J. Lagowski (Marcel Dekker, New York, 1977), Chaps. 9 and 10, pp. 352–452.

[13]See, for example, H. C. Van der Hulst, *Light Scattering by Small Particles* (Dover, New York, 1967), Chap. 7, pp. 88–92.

[14]J. W. Vanderhoff, H. J. Van den Hull, R. J. Tavsk, and J. Th. G. Overbeek, in *Clean Surfaces: Their Preparation and Characterization for Interfacial Studies,* edited by G. Goldfinger (Marcel Dekker, New York, 1970), pp. 21–24.

[15]M. L. Broide, Ph.D. thesis, Massachusetts Institute of Technology, 1988 (unpublished).

[16]M. E. Fisher and R. J. Burford, Phys. Rev. A **156**, 583 (1967).

[17]MINUIT (FORTRAN, 2891 cards); F. James, M. Ross, Comput. Phys. Commun. **10**, 343 (1975).

[18]M. Matsushita, K. Sumida, and Y. Sawada, J. Phys. Soc. Jpn. **54**, 2786 (1985).

[19]D. A. Weitz (private communication).

[20]R. Jullien, Phys. Rev. Lett. **55**, 1697 (1985).

[21]R. Jullien, J. Phys. A **19**, 2129 (1986).

[22]A. Hurd and D. Schaefer, Phys. Rev. Lett. **54**, 1043 (1985).